

**Progress Report FY87:
Development of TiN Low-Emissivity Coatings**

M. Rubin

Windows and Daylighting Group
Lawrence Berkeley Laboratory
University of California
Berkeley, California 94720

ABSTRACT

Titanium nitride (TiN) shows promise as a low-emittance coating for windows because it possesses both the optical properties of a metal and the hardness and inertness of a ceramic. Titanium dioxide (TiO₂) is a convenient choice for a matching layer to enhance the solar transparency. TiN and TiO₂ films have been deposited on glass by reactive dc magnetron sputtering, which is a standard technique used for production of window coatings. The composition of these films was determined by X-ray photoelectron spectroscopy (XPS). Incorporation of N and O appears to follow the Langmuir adsorption isotherm at low partial pressures. Structure was determined by x-ray diffraction, using both Seemann-Bohlin and conventional Bragg-type geometries. Nonequilibrium phase diagrams have been prepared from this information for various deposition conditions. The properties of these films depend strongly on the sputtering conditions, especially gas pressures, substrate temperature, and bias voltage. Emittance values have been achieved that are much lower than those of TiN films produced commercially. Multilayer coatings have been deposited with greatly improved spectral selectivity.

December 8, 1987

Progress Report FY87:
Development of TiN Low-Emissivity Coatings

M. Rubin

Windows and Daylighting Group

Lawrence Berkeley Laboratory

University of California

Berkeley, California 94720

Introduction

A "low-emittance" coating is a type of spectral filter that has a high transmittance τ in the visible or solar spectrum and a high reflectance ρ (low emittance ϵ) in the thermal infrared. When deposited on a window surface the low- ϵ coating suppresses radiative heat transfer and thereby improves the thermal insulating value of the window. TiN shows promise for this application because it combines optical properties similar to those of the metals often used in low- ϵ coatings with the better mechanical and chemical resistance of a ceramic. Currently manufactured TiN films, however, have a relatively high emittance. In this report we present the results of our work to lower the emissivity of TiN films and to design a TiN-based low- ϵ multilayer

Lifetime is a major concern for coatings applied to windows that should survive for decades. Sputtered metal-based coatings have become known as "soft coats" in unfavorable comparison to oxide "hard coats" deposited by pyrolysis. A properly grown TiN film will be much harder and more chemically inert than a metal film. The adhesion of the film will depend on the interaction between the film and substrate. Most studies of

the mechanical properties of TiN coatings have been performed with steel substrates rather than glass. We have not yet performed accelerated weathering tests on our sputtered films. We have observed, however, that the optical properties of these TiN films are much more stable than those of silver films when exposed to air at temperatures of 150 C even for 24 hours. Also, TiN coatings are used as solar control coatings on monolithic glass, indicating that they are more durable than sputtered silver low- ϵ coatings.

First, we briefly describe the process used to grow TiN films and the techniques used for characterizing composition and optical properties. Then, we present the optical properties of films and multilayers as related to low- ϵ applications.

Deposition Process and Characterization

All films were deposited by d.c. reactive magnetron sputtering. This is essentially the same process used in large scale commercial deposition of window coatings. TiN films were grown on glass substrates by sputtering from a Ti target in Ar mixed with N₂. TiO₂ was a convenient choice for antireflecting layers because of its high index and the fact that it can also be sputtered from the Ti target. In the case of TiO₂, pure Ar was mixed with 2% O₂/98% Ar to achieve finer control over O₂ flow rates. The substrates were heated to temperatures up to 500 C. Without heating the film temperature reached only 50-60 C. In some cases a bias of 100 Volts was applied to the substrate.

In a later section, we will discuss the effect of specific deposition parameters on the resulting film. For the present, it will be convenient to anticipate that we can grow films with a variety of compositions and structures. Many films and crystals of supposedly near-stoichiometric "TiN" have been grown by a variety of methods. Measurements of optical properties, even for films grown under similar conditions, yield disparate results. Toth [1] believes that many of the measured physical properties of TiN are in error because the tendency of this material to be nonstoichiometric makes determinations of

composition uncertain.

Two techniques for quantitative analysis were tried and rejected. Rutherford back-scattering spectrometry (RBS) was unsuitable because the high energy ions penetrate up to a few microns into the glass substrate. Silicon in the thick glass obscures the signal from the lighter elements in the film. The large sampling depth also prevents the use of depth profiling. Auger electron spectroscopy (AES) likewise proved unsatisfactory. In AES the only N peak coincides in energy with the strongest Ti peak. Sundgren [2] utilized the fact that the N signal has practically no negative excursion in order to deconvolute this peak. This approach, however, was found to be insufficiently accurate for our purposes.

We turned to X-ray photoelectron spectroscopy (XPS) because the N and Ti peaks do not overlap. Furthermore, a high-resolution XPS spectra carries information about the chemical state of the element, whereas AES usually gives only the concentration. XPS, however, is less convenient than AES because the spectra take longer to attain the same signal-to-noise level. Figure 1 shows a typical XPS spectrum from the surface of a TiN film. The principal peaks of interest are the Ti $2p_{3/2}$ (458 eV), N $1s$ (402 eV), and O $1s$ (531 eV). Other peaks that appear are the C $1s$ (287 eV) and Ar $2p_{3/2}$ (241 eV). The C signal disappears in all cases after sputtering away 20 Å of the surface. The O peak diminishes greatly in most cases while the Ar diminishes slightly beneath the surface. Figure 2 shows high-resolution XPS spectra of the Ti peak in this film. In Fig. 2a the spectrum is taken from the surface of the film as deposited. The peak energy is about 458 eV, characteristic of Ti^{4+} in TiO_2 [3]. After sputtering to a depth of 2 nm Fig 2b shows that the peak shifts to 454 eV as in TiN [4].

Standards, either in bulk or thin-film form, were difficult to obtain and certify. We used the fact that certain known line compounds or stoichiometric compositions along

the boundaries of the phase triangle had extremum values of electrical resistivity or lattice parameters. The resistivity and d-spacings could be measured very precisely and thus used to fix the sensitivity factors of the elements.

These ratios are assumed to vary linearly between calibration points. This assumption will certainly be good in the two-phase regions where the amount of the two limiting phases changes linearly. In the broad single-phase regions, such as α -Ti and δ -TiN, deviations from linearity are more likely. In the case of oxynitrides, it would be simplest to treat the oxide and nitride calibration factors as being independent. This approach would be partly justified if there were very little interaction between the non-metal atoms. At least in the case of TiN_x and TiO_y this assumption is supported by theoretical and experimental results. Rundle [5], Kiessling [6] and others claim that bonding in these materials is primarily metal-metal and metal-nonmetal.

The phases present in the film are determined by x-ray diffraction. Two techniques are used: a conventional Bragg-type diffractometer and a Seemann-Bohlin diffractometer. The first arrangement sees only those planes that are parallel to the surface of the film because the goniometer drive is coupled in the usual θ - 2θ condition. The Seemann-Bohlin arrangement, on the other hand, allows independent motion of the source and detector. In particular, the source is set to a fixed low angle of incidence (e.g., 6°) and the detector moves through a wide range. The low angle makes this technique more sensitive to the surface which is helpful for studying thin films. Also, the ability to see planes off parallel is very important because many vacuum deposited thin films grow with a strong preferred orientation.

Figure 3 shows a Seemann-Bohlin diffractogram of nearly stoichiometric TiN. Despite the fact that the film is only 200 Å thick the peaks were clearly resolved in less than 3 sec. per channel. All allowed fcc peaks appear, as labeled, indicating that the

film is randomly oriented. Figure 4 shows a similar diffractogram of TiO_2 . The pattern is that of the anatase form which has a tetragonal lattice.

Using the methods described above, we can in principle find the location of any film in the composition space and index it according to the phases present. This information together with thermodynamically derived rules for drawing phase boundaries and some foreknowledge from the literature will allow us to construct useful phase diagrams.

Phase Diagrams

Stone [7] constructed the only known phase diagrams for the ternary system. They were limited, however, to the Ti-rich portion (0-7% N or O) and to very high temperatures (1000, 1400 °C). The binary Ti-O, and, to a lesser extent, the Ti-N phase equilibria have been studied over a wide range of temperature: Bumps [8], DeVries [9], and Wahlbeck [10] constructed Ti-TiO₂ diagrams from room temperature to the melting point. These diagrams were composites that attempted to integrate several previous investigations covering narrower composition ranges. This system is quite complex and there are major discrepancies between each of the above mentioned diagrams. The range, structure, and even the existence of several phases is in doubt. Palty [11] and recently Molarius [12] completed similar works for the Ti-TiN system. The studies mentioned above pertain to bulk crystals. Isolated phases have been identified in various thin films, but no systematic attempt has been made to construct a phase diagram.

Originally, this work began as an attempt to make a gradient index optical coating that varied continuously from TiN to TiO. Little was known about TiO and it was widely assumed to be a dielectric and to be isomorphous with TiN. During the course of our experiments we discovered that TiO was not dielectric, but, like TiN, a metallic compound [13]. Furthermore, TiO does not have the same structure as cubic TiN; ordered vacancies in TiO result in a monoclinic lattice [14]. Subsequently, we shifted our

attention to composite films of TiN and TiO₂. In the process we produced hundreds of thin films having various compositions within the Ti-N-O system. Ternary phase diagrams are constructed from the accumulated data on elemental and phase composition.

A series of sputtered films of various compositions have been prepared at substrate temperatures of 60, 150, and 500 °C and at 60 C with -100 V of bias. The lowest temperature is typical of samples that are not heated except by the unavoidable electron bombardment from the discharge; industrial coaters do not have substrate heating. The middle temperature is the highest practical temperature that could be achieved without a major redesign of the large-scale industrial coater [15]. The highest temperature is chosen to be safely below the softening point of window glass [16]. Modification of industrial coaters to allow substrate heating could greatly improve film quality. The application of a bias voltage is an alternative to heating that may be easier to implement.

Figure 5 shows the high-temperature (500 C) ternary phase diagram. Although these diagrams resemble conventional ternary phase diagrams, they do not necessarily represent near-equilibrium conditions. Thus, they should not be thought of as isothermal sections, but rather as representing a specific set of deposition conditions including the substrate temperature. Despite this caution, when a feature of the diagram is uncertain, the position of the phase boundaries are drawn in accordance with the thermodynamic rules governing equilibrium diagrams (e.g., contact rule, curvature rule).

The most notable feature of Fig. 5 is the existence of the broad single-phase δ -TiN region having the NaCl structure. TiN is known to be a "defect" compound which can have a high fraction of nitrogen sites vacant. Below stoichiometry the N atoms are arranged randomly on their sublattice. Above stoichiometry, vacancies appear on the Ti

sublattice. TiO_2 has a much narrower range of stability, but is still apparently a defect compound. Unlike TiN, however, TiO_2 cannot be overstoichiometric, which greatly simplifies the process of making a stoichiometric compound.

There is also an α -Ti solid solution with the hexagonal close-packed structure. On the Ti-N side, we find only one other line compound, ϵ Ti_2N , in accordance with the findings of Nowotny [17] and Holmberg [18]. On the Ti-O side we also find a known line compound, Ti_2O_3 , but a number of other compounds noted on the margin of the diagram are not found. Note that the δ phase extends across the entire diagram, but does not encompass stoichiometric TiO as it does TiN. At 50 % oxygen, there are ordered vacancies on both sublattices resulting in a monoclinic structure. As the oxygen content increases, the vacancies are on the Ti sublattice and disordered, returning to the NaCl structure.

The phase diagram of the unheated samples is relatively featureless. The single-phase α and δ regions still exist, but the two-phase $\alpha+\epsilon$ and $\epsilon+\delta$ regions are not observed. These regions are separated by the ϵ line near the Ti-N edge. Two phase regions must exist in equilibrium because the transformation from α to δ cannot be 1st order. These regions, however, may be extremely narrow under these conditions, or, more likely, they are amorphous. In the vicinity of the TiO_2 composition an amorphous material appears with a broader extent than in the higher temperature case. Chemically, these films are still TiO_2 as shown by the position of the Ti peak in XPS and by infrared spectroscopy.

Composition Control

The phase diagrams discussed above provide us with a map of our materials system. Although these diagrams are useful guides they say nothing about the specific sputtering conditions required to obtain a particular film composition or structure. A

comprehensive analysis of the growth parameters is being prepared for a technical paper. Here we attempt to adapt a simple theory for the adsorption of gases to the incorporation of reactive species in growing films.

The arrival rate of Ti atoms at the substrate is primarily determined by the power applied to the target and the total pressure P . The pressure affects the plasma impedance which determines how the available power appears as voltage and current. Increasing the current generally has a much stronger influence on sputtering rate. Let us assume that these variables remain fixed despite small changes in other system parameters.

The Ti atoms arriving at a constant rate can be viewed as providing a continuously renewed clean surface with vacant sites for adsorption of the nonmetal atoms. For a single reactive gas species A , the fraction of occupied non-metal sites is proportional to the rate of impingement (proportional to its partial pressure P_a) and the probability that a site is vacant ($1-C_a$):

$$C_a = a P_a (1-C_a) \quad (1)$$

where a depends on temperature T and the sticking probability of an atom incident on a vacant site. Thus, for a given material at constant T , a is constant. Rearranging Eq. (1) yields the Langmuir adsorption isotherm,

$$C_a = \frac{a P_a}{1 + a P_a} \quad (2)$$

which predicts that the concentration of in the film increases hyperbolically with pressure. Thus, because it is assumed that only one atom can be adsorbed per site, the concentration approaches a limiting value.

We can extend this concept to the case of two gas species, A and B . The probability of an empty site is now $1-C_a-C_b$, giving

$$C_a = a P_a (1 - C_a - C_b) \quad (3)$$

and

$$C_b = b P_b (1 - C_a - C_b) \quad (4)$$

Rearranging Eqs. (3) and (4) gives,

$$C_a = \frac{a P_a}{1 + a P_a} (1 - C_b) = X_a (1 - C_b) \quad (5)$$

and

$$C_b = \frac{b P_b}{1 + b P_b} (1 - C_a) = Y_b (1 - C_a). \quad (6)$$

Combining Eqs. (5) and (6) gives C_a in terms of the partial pressures:

$$C_a(P_a, P_b) = \frac{X_a (1 - X_b)}{1 - X_a X_b}. \quad (7)$$

As $P_a \rightarrow 0$, $C_a \rightarrow 0$; as $P_b \rightarrow 0$, $C_a \rightarrow X_a$, i.e., we return to a simple hyperbolic dependence on pressure as in Eq. (2). A large value of P_b extends the near-linear portion of the curve (Henry's Law) to larger P_a .

In Figure 6 we show the results of fitting Eq. (2) to our data by adjusting the parameter a . For small values of P_{N_2} experimental and calculated values agree well. As P_{N_2} increases, however, C_N suddenly exceeds the predicted values. This phenomenon can be explained by the formation of a compound on the target surface which causes the sputtering rate to drop. Thus the arrival rate of Ti drops and some N now arrives directly from the target. The concentration of N in the films rapidly increases beyond the transition point, filling the remaining vacancies. As previously noted, TiN_x films can be overstoichiometric if P_{N_2} is high.

Optical Properties of TiN Films

The spectral transmittance τ and reflectance ρ of all films produced in this work were measured over a wide spectral range. In the ultraviolet, visible, and near-infrared, a scanning spectrophotometer (Perkin-Elmer model Lambda 9) was used with a Strong-type absolute reflectometer. In the middle to far infrared a Fourier-transform spectrophotometer (Mattson model Sirius 100) was used with a freshly deposited Al reflectance standard. Visible, solar, and infrared averages (e.g., ρ_s , ρ_v , ρ_{ir}) were calculated from the spectral quantities weighted by the color-corrected visible, solar, and thermal infrared sources. Optical constants were determined in the visible using an automatically compensated scanning ellipsometer. Outside this region optical constants were determined either by Kramers-Kronig analysis or by inversion of the photometric properties.

Optically thick films of TiN can be classified by the shape of their reflectivity spectrum. For use as a transparent low- ϵ coating the reflectivity should be as high as possible in the infrared and have a sharp cutoff towards the visible. Poltis [19] grew single crystals of TiN by chemical vapor deposition at temperatures between 1940 and 2460 °K. This material more closely approaches the ideal than any other yet reported in the literature. The growth temperature, however, is far too high to consider for deposition on glass. In Fig. 7 the the crystals made by Poltis are designated as Type I. Bohm [20], Knosp [21] and Schlegel [22] prepared single crystal specimens by other methods, but their reflectivity was not nearly as high as the crystals of Poltis. This fact reminds us to be careful in characterization of this defect compound and not to assume that a bulk sample can be used as a standard of purity.

Small deviations from stoichiometry and crystallinity result in large changes in reflectivity. We identify four characteristic spectra that result from identifiable defects. The Type II spectrum of Fig. 7 represents our best sputtered films. The ρ_{ir} is lower and

the edge is less sharp than Type I. These films were grown at a substrate temperature of 500 C and were determined to be nearly stoichiometric. Similar properties were observed for films grown at 60 C with -100 V bias. Unlike the Type I single crystal, Type II films are polycrystalline and undoubtedly contain more oxygen, carbon, and argon.

Too little nitrogen or too much nitrogen in the material further degrades ρ_{ir} and softens the edge in slightly different ways. These are referred to in Fig. 7 as Type III and Type IV films, respectively. Substoichiometric Type III films are blue-shifted from Type II films, whereas superstoichiometric Type IV films are red-shifted. A continuous variation in optical properties occurs between Type III and Type IV films with a maximum infrared reflectivity occurring for Type II films. The violet reflectance of the Type IV films tends to be less than Types II and III.

A fifth category of film can be defined as having substitutional oxygen or carbon in place of nitrogen. These impurities may have their source in the residual gases in the sputtering system or they may be incorporated into a porous film after exposure to the atmosphere. Fig. 7 shows that such films, designated Type V, have a red shift similar to Type IV except for a higher reflectance in the violet. Bohm [20], Knosp [21], Karlsson [23], and Roux [24] showed this trend for titanium carbonitrides. We did not intentionally introduce carbon, but our oxynitride films show a similar spectral shift. Most results reported in the literature [20-22,24,25] indicate films with Type III, IV, and V defects. Only Karlsson [23] appears to have produced films with the high reflectivity characteristic of Type II films.

In principle, we can use the optical constants of these films to calculate the properties of similar films of different thickness on other substrates. Similarly, the properties of thin-film multilayers are calculated from optical constants. Three methods are used to

determine optical constants: ellipsometry, Kramers-Kronig analysis, and inversion of the photometric properties. Ellipsometry is the most accurate technique that is available to us, but our equipment only covers the visible spectrum. Like the reflectivity spectrum, the optical constants are similar to those of a noble metal. These values are used to calculate the theoretical photometric properties presented below.

As the thickness of the film decreases, ρ_{ir} decreases (ϵ_{ir} increases) while τ_s and τ_v increase. This trade-off is shown in Figs. 8a and 8b. The ideal coating would have $\tau_{v,s}=1$ and $\rho_{ir}=1$ in the upper right hand corner of Fig. 8a or 8b. Calculations of photometric properties are performed using the optical constants derived from optically thick films and then compared to experimental results for thinner films. Valkonen [26] observed a strong dependence of the optical constants on thickness. In accordance with that result, we find that ρ_{ir} , and, to a lesser extent, τ_s and τ_v deviate increasingly from the predicted values as thickness diminishes. This deviation can be greatly reduced by heating to 500 C. Heating to 150 C, however, has a relatively small stabilizing effect. Currently manufactured solar control coatings fall well below even the 60 C points.

The metal layer of a low- ϵ coating is often sandwiched between two dielectric layers to enhance τ_v or τ_s . In Figs. 8a and 8b we also show the properties of multilayers with the following structure: $TiO_2/TiN/TiO_2/glass$. The thickness of the TiO_2 layers is optimized to give maximum τ_v or τ_s at a given TiN thickness. Also shown for comparison are values for typical sputtered silver and pyrolytic low- ϵ coatings.

Discussion and Conclusions

TiN films have been deposited by sputtering under laboratory conditions that have emissivities significantly lower than those produced in standard commercial practice. When incorporated into a multilayer coating this material has optical selectivity approaching other low- ϵ coatings. The hardness and chemical resistance of TiN is at the

same time far superior to the silver films often used in this application. To produce such films in quantity, however, would require modifications to current standard equipment.

At low temperature (60 C), the nitrogen flow rate must be precisely controlled to produce stoichiometric TiN. Even small fluctuations in other sputtering parameters, such as the applied power, may cause the composition to deviate enough to significantly reduce ρ_{ir} . Under these circumstances, current industrial sputtering technology cannot be expected to repeatably produce Type II films. The most convenient mode of operation at low temperature is well above the transition point where an overstoichiometric film can be produced repeatably. Optically, however, such films will be far from optimum. Also, the sputtering rate will fall well below the pretransition (metal-sputtering) value.

The higher the growth temperature, the greater the tendency towards stoichiometry. At 500 C good optical quality could be achieved routinely, but even the more modest goal of 150 C might allow better quality films. Substrate bias could be used as an alternative to heating, but would also require modifications to an industrial sputtering system. These issues will be pursued through discussions with manufacturers.

Acknowledgement

This work was supported by the Assistant Secretary for Conservation and Renewable Energy, Office of Buildings and Community Systems, Buildings Systems Division of the U.S. Department of Energy under Contract No. DE-AC03-76SF00098.

References

1. L.E. Toth, "Transition-Metal Carbides and Nitrides", Academic Press, New York (1971).

2. J.-E. Sundgren, *Thin Solid Films* 105 (1983) 353.
3. L. Porte and M. Demosthenous, *J. Less Common Metals* 56 (1977) 183.
4. L. Ramquist, et al., *J. Phys. Chem. Solids* 31 (1969) 1835.
5. R.E. Rundle, *Acta Crysta.* 1 (1948) 180.
6. R. Kiessling, *Met. Rev.* 2 (1957) 77.
7. L. Stone and H. Margolin, *J. Metals* 5 (1953) 1498.
8. E.S. Bumps, H.D. Kessler, and M. Hansen, *Trans. Am. Soc. Metals* 45 (1954) 1013.
9. R.C. DeVries and R. Roy, *Ceramic Bull.* 33 (1954) 370.
10. P.G. Wahlbeck and P.W. Gilles, *J. Am. Ceramic Soc.* 49 (1966) 180.
11. A.E. Palty, H. Margolin, and J.P. Nielsen, *Trans. Am. Soc. Metals* 46 (1954) 312.
12. J.M. Molarius, A.S. Korhonen, and E.O. Ristolainen, *J. Vac. Sci. Technol.* A3 (1985) 2419.
13. A. Neckel, et al., *J. Phys C: Solid State Phys.* 9 (1976) 579.
14. D. Watanabe, J.R. Castles, A. Jostsons, and A.S. Malin, *Acta Cryst.* 23 (1967) 307.
15. S. Nadel, Airco Solar Products, private communication.
16. P. Reid, Ford Motor Co., Glass Division, private communication.
17. H. Nowotny, et al., *Monatsh. Chem.* 92 (1961) 403.
18. B. Holmberg, *Acta Chem. Scand.* 16 (1962) 1255.
19. C. Poltis, Th. Wolf, and H. Schneider, *Proc. 7th Int. Conf. on Chemical Vapor Deposition* (1979) 289.
20. G. Bohm and H. Goretzki, *J. Less-Common Metals* 27 (1972) 311.
21. H. Knosp and H. Goretzki, *Z. Metallkde.* 60 (1969) 587.

22. A. Schlegel, et al., J. Phys. C: Solid State Phys. 10 (1977) 4889.
23. B. Karlsson, J.-E. Sundgren, and B.-O. Johansson, Thin Solid Films 87 (1982) 181.
24. L. Roux, et al., Solar Energy Mater. 7 (1982) 299.
25. J. Rivory, et al., Thin Solid Films 78 (1981) 161.
26. E. Valkonen, C.-G. Ribbing, and J.-E. Sundgren, Appl. Opt. 25 (1986) 3624.

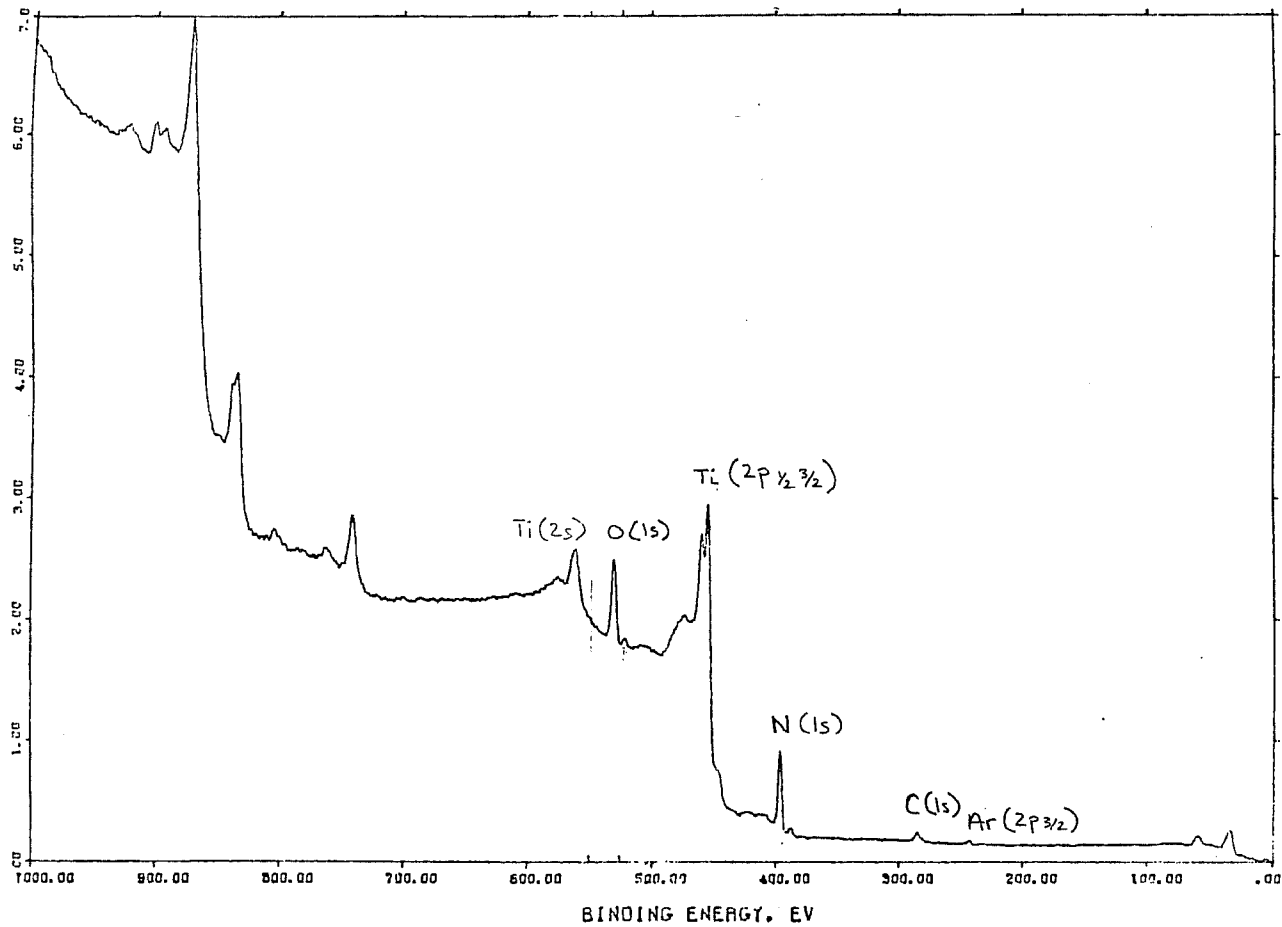


Figure 1. X-ray photoelectron spectrum of titanium oxynitride sputtered film

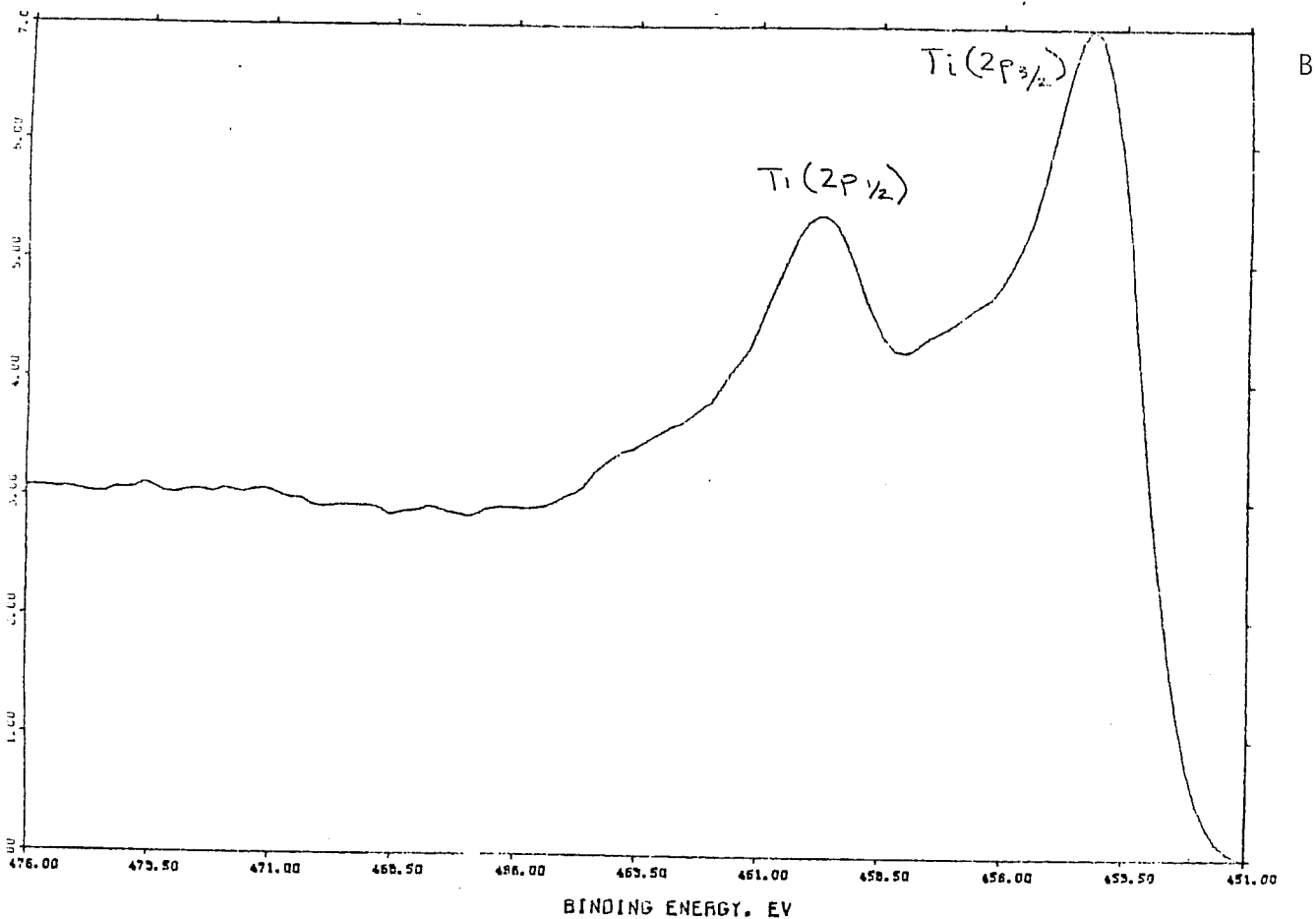
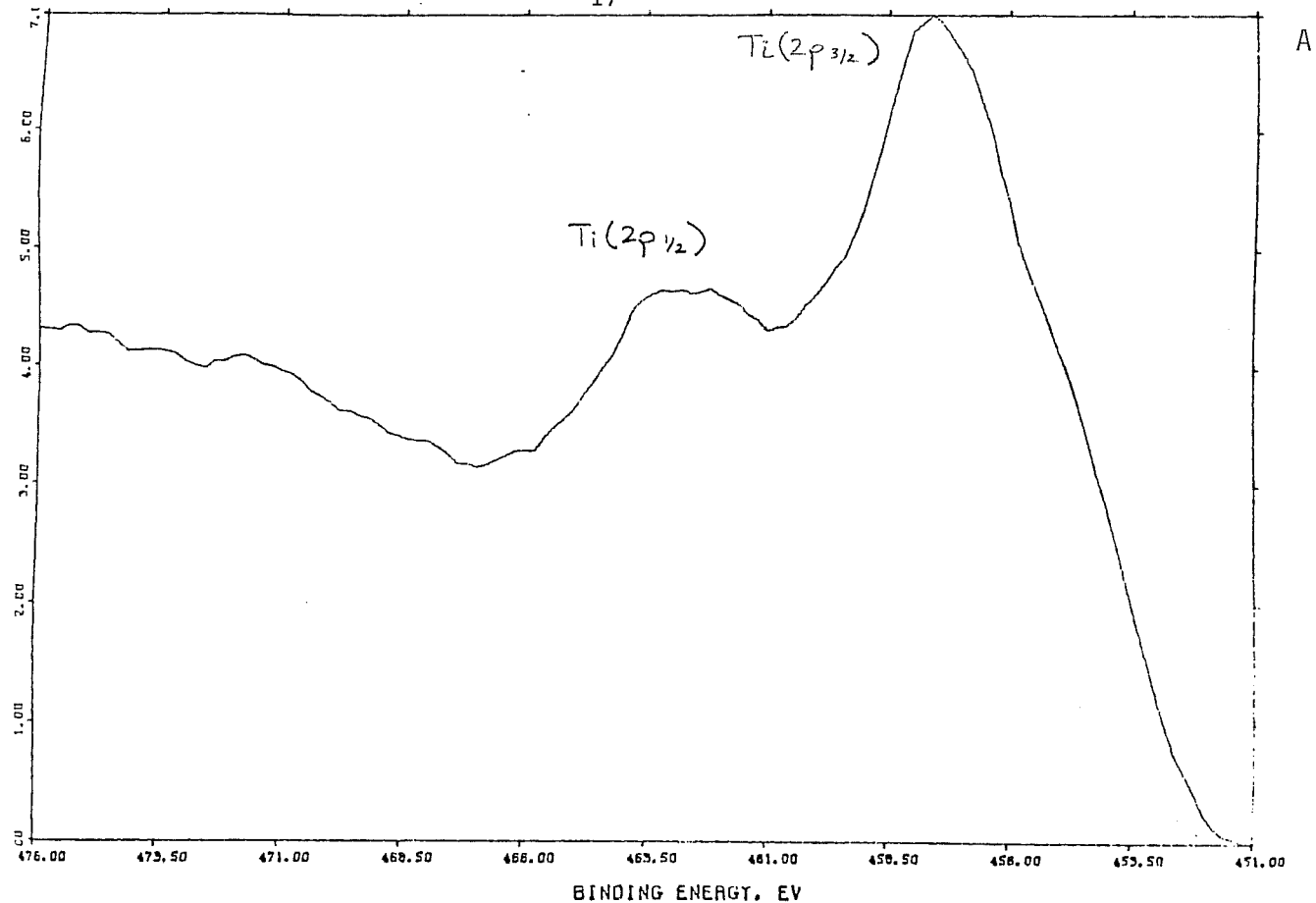


Figure 2. High-resolution x-ray photoelectron spectrum of the Ti 2p_{3/2} peak in a titanium oxynitride sputtered film: a) from the surface of the film as deposited; b) from 20 nm below the film surface.

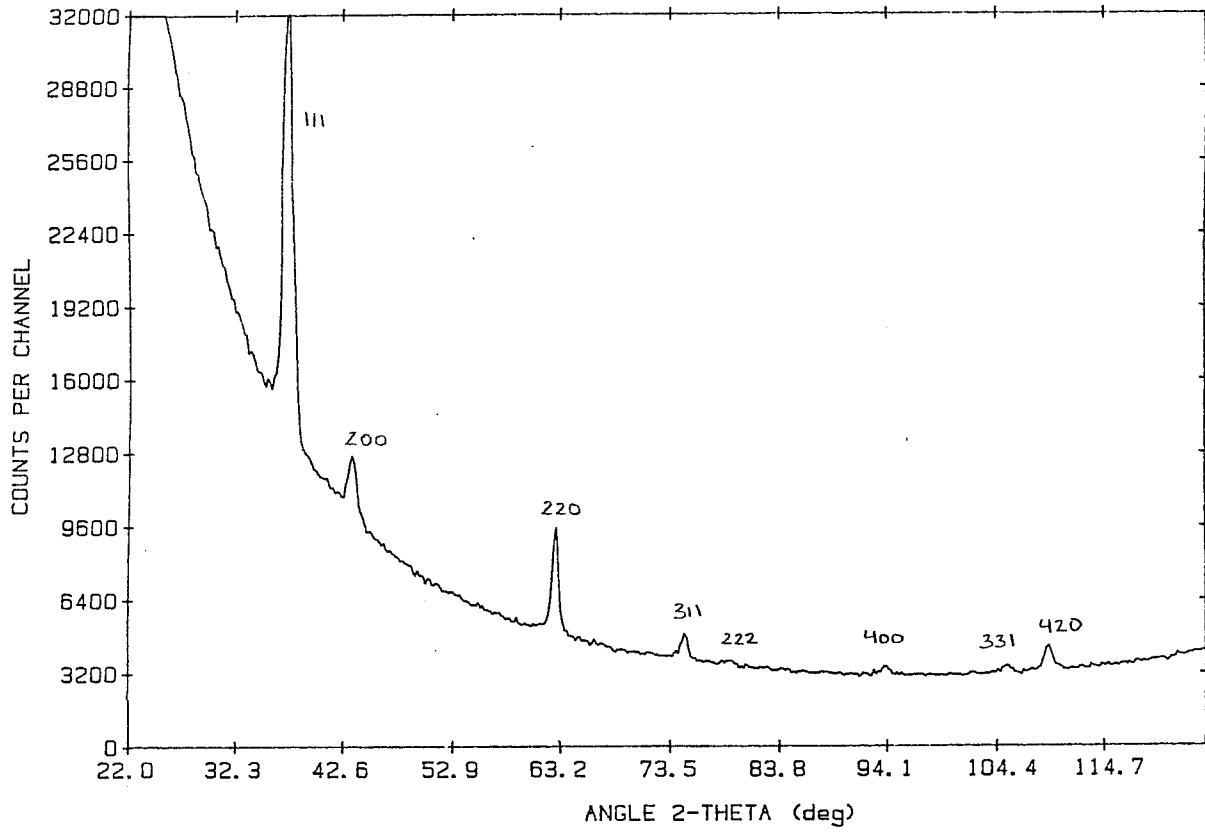


Figure 3. Seemann-Bohlin x-ray diffractogram of a δ -TiN film having the NaCl cubic structure.

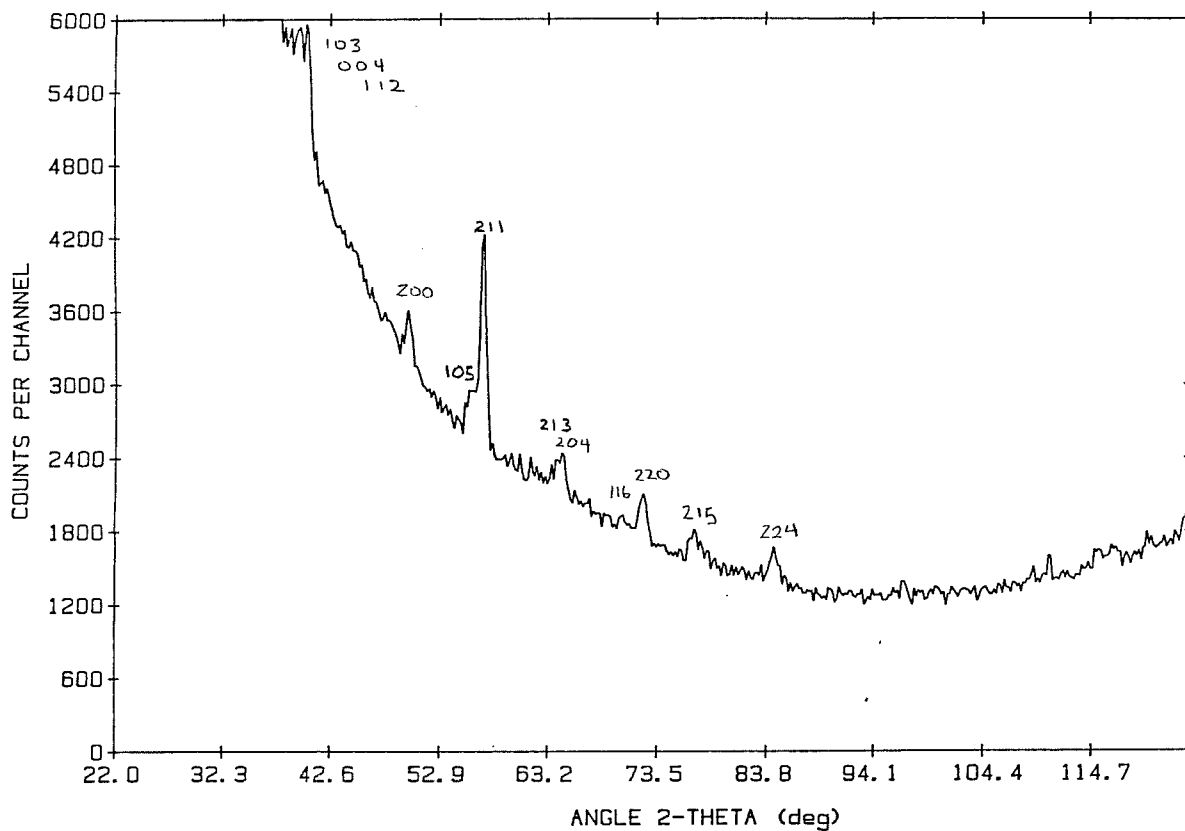


Figure 4. Seemann-Bohlin x-ray diffractogram of a λ -TiO₂ film having the anatase tetragonal structure.

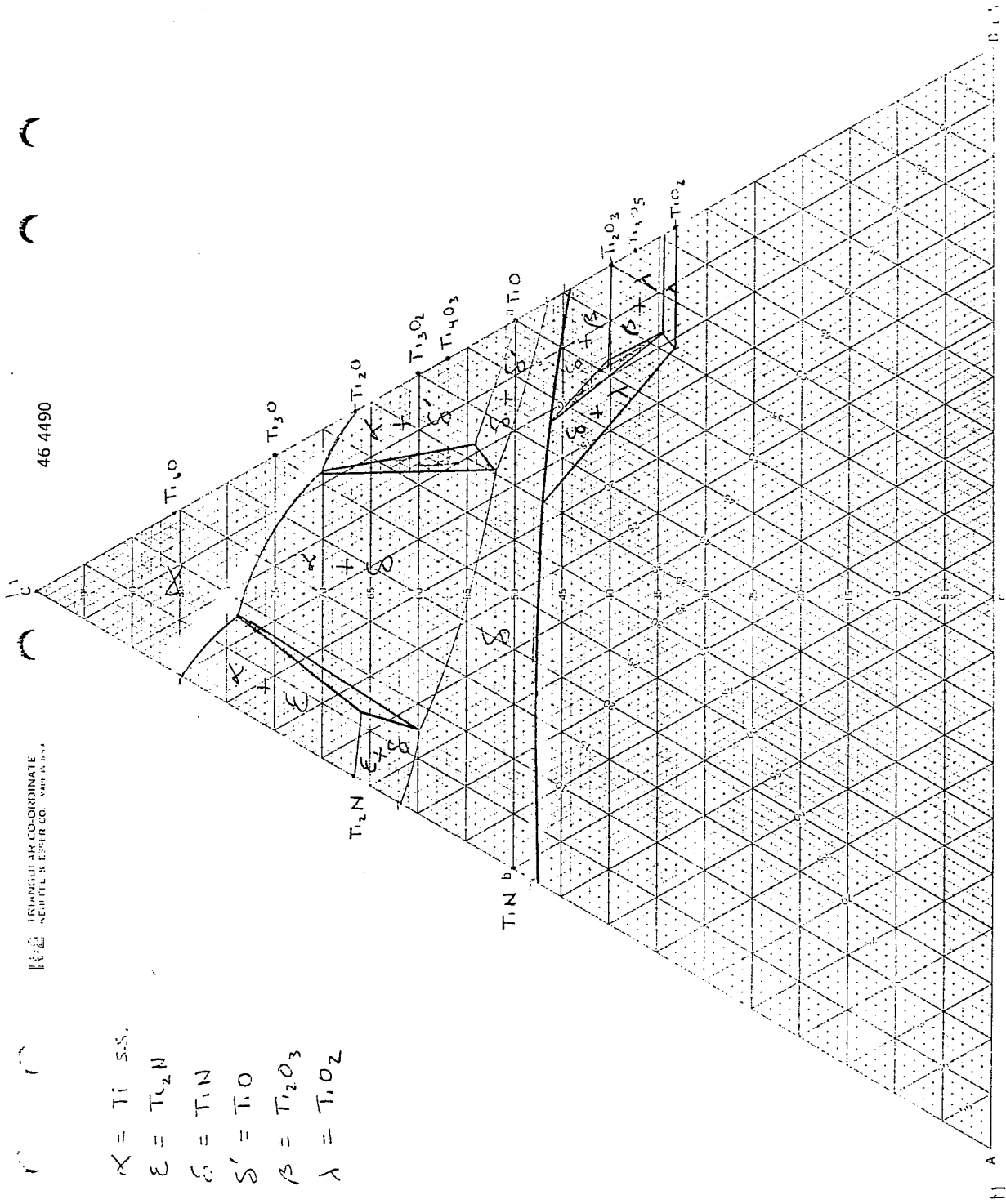


Figure 5. Ternary phase diagram of the Ti-N-O system for the near-equilibrium case of films sputtered at 500 C.

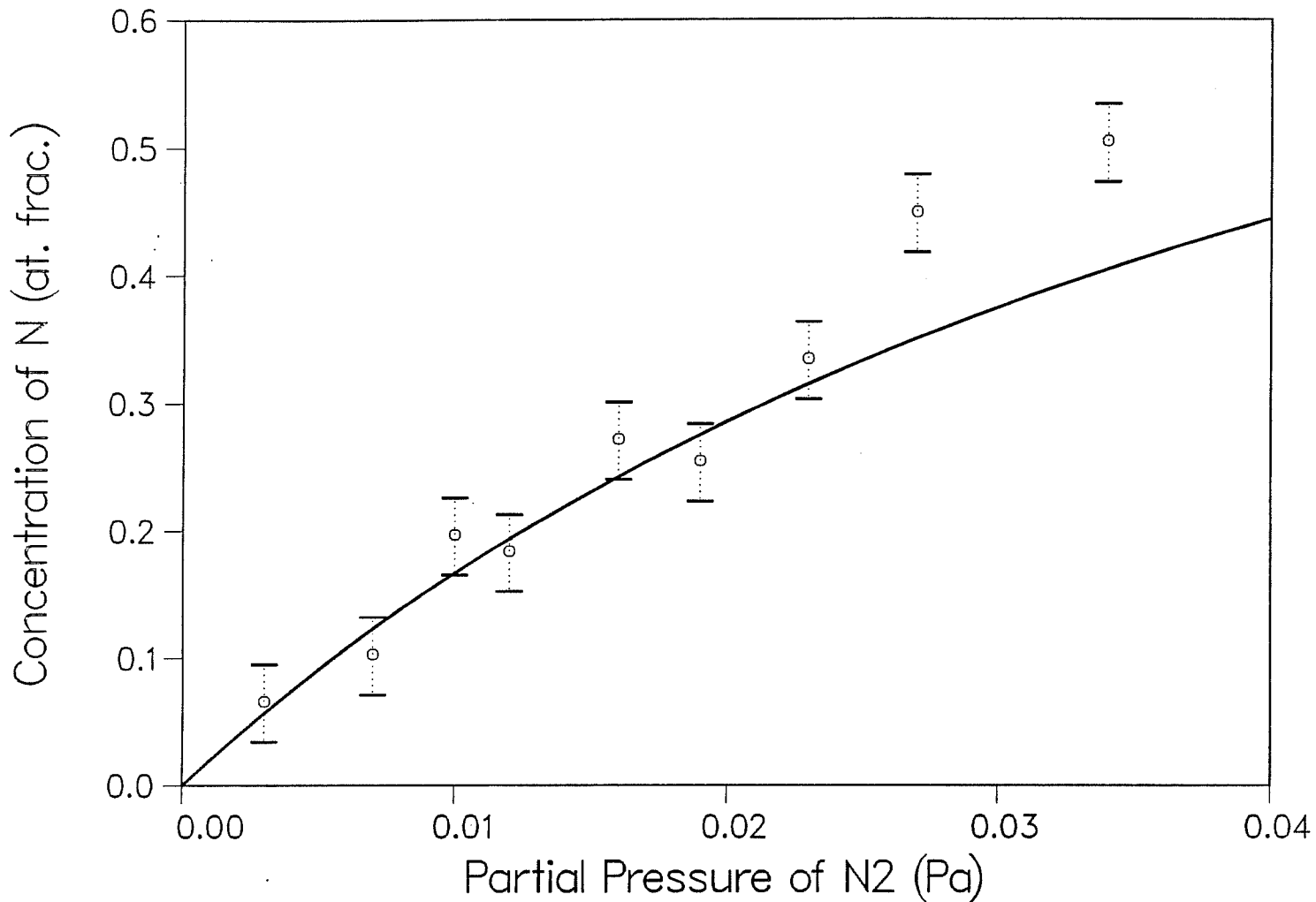


Figure 6. Nitrogen concentration in a sputtered film versus the nitrogen partial pressure. The curve fits the Langmuir desorption isotherm to the points below the target transition.

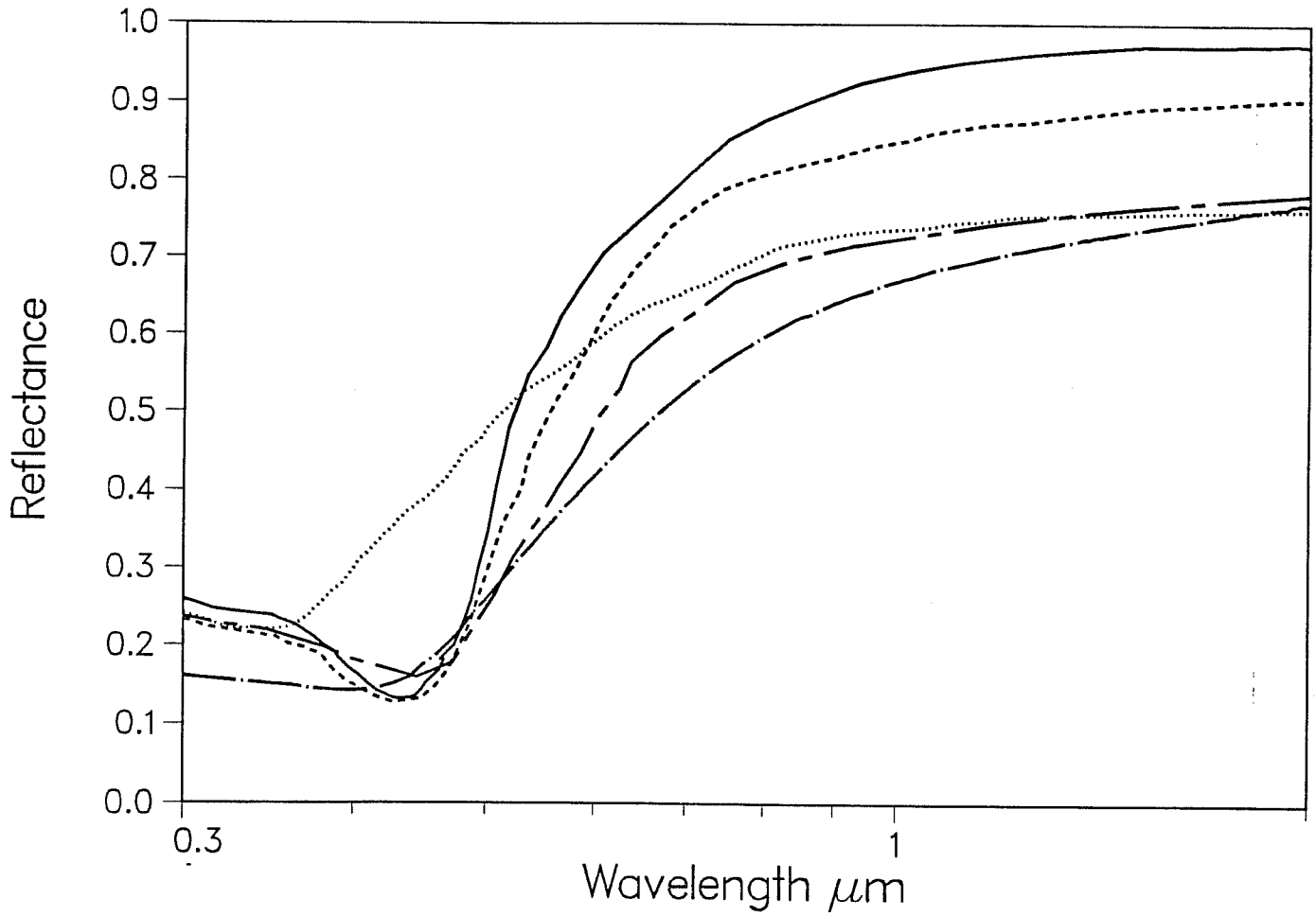


Figure 7. Solar spectral reflectivity of thick TiN films. — Type I, single crystal from [19]; --- Type II, sputtered, nearly stoichiometric; ... Type III, sputtered, understoichiometric; .— Type IV, sputtered, overstoichiometric; _ _ Type V, sputtered, oxygen substitution.

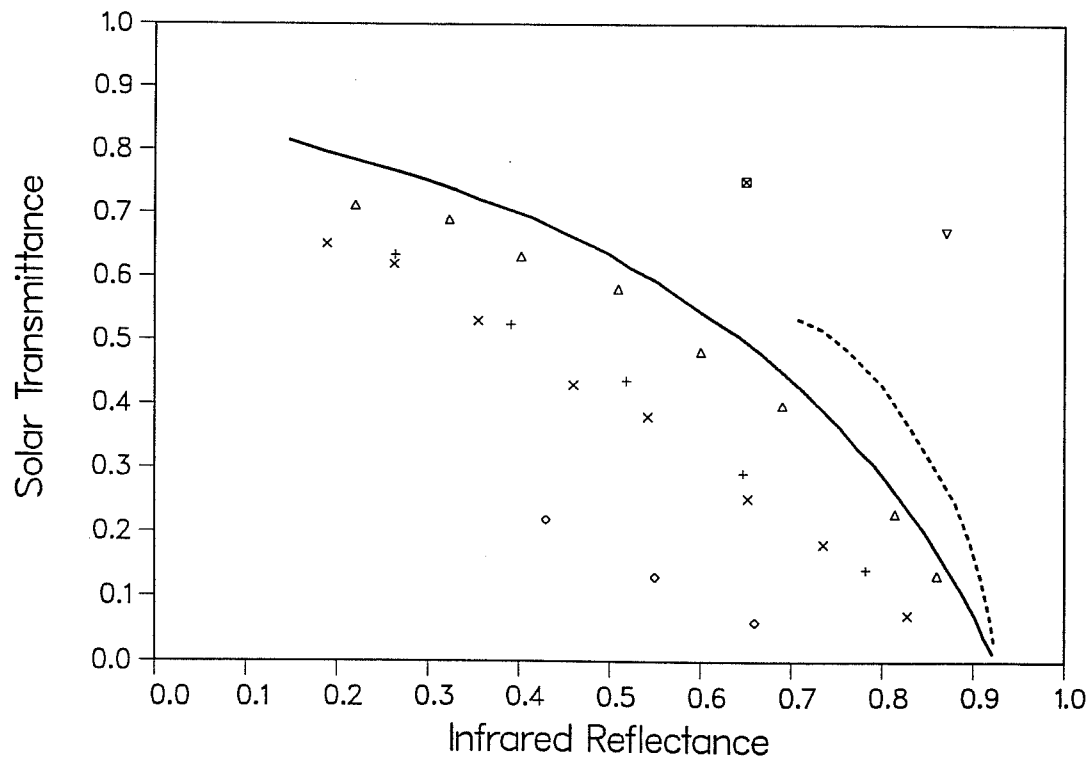
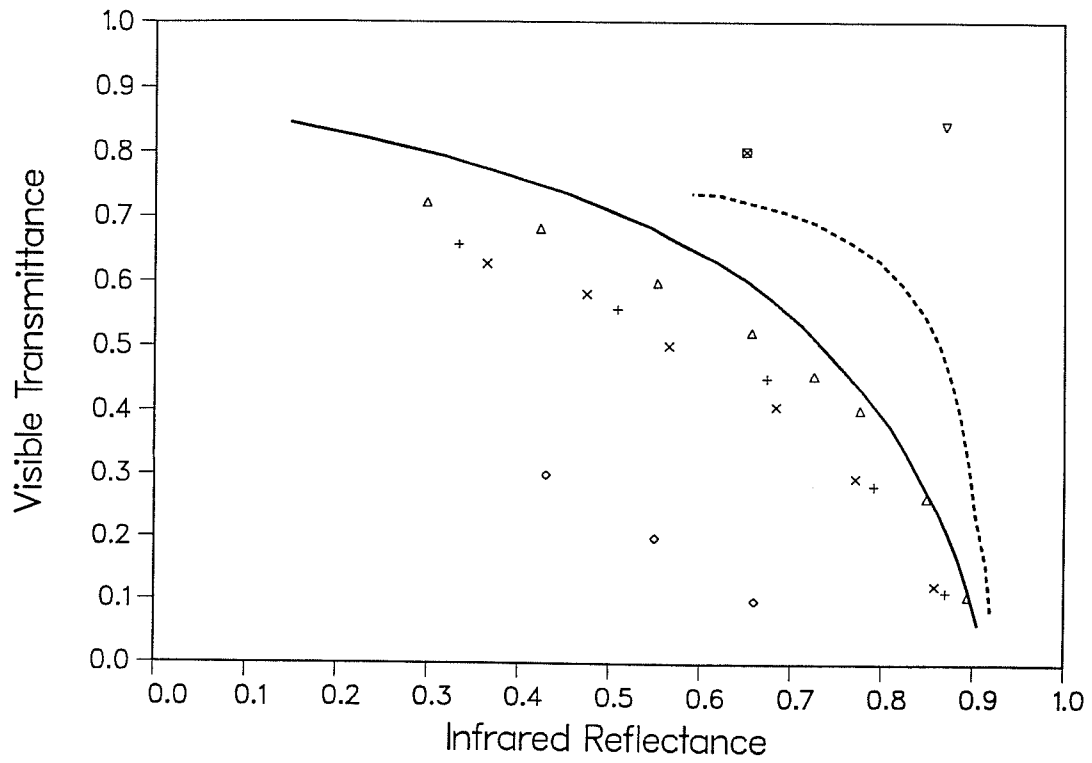


Figure 8. Comparison of low- ϵ coatings: a) visible transmittance and b) solar transmittance versus infrared reflectance for ___ TiN films, calculated; --- TiN/TiO₂ multilayers, calculated; Δ 500 C; + 150 C; \times 60 C; \diamond commercial sputtered TiN solar control films; ∇ commercial sputtered silver-based multilayer; \boxtimes commercial pyrolitic SnO₂ thick film.